Band Gap Size Dependence of Topological Insulator Bi_2Te_3 Nanotube

Igor BEJENARI, Valeriu KANTSER
Institute of Electronic Engineering and Nanotechnologies "D.Ghitu", ASM
bejenari@iieti.asm.md

***Abstract* — We study the electronic structure of a cylindrical nanotube made of a topological insulator Bi_2Te_3. The calculation was made in the framework of the *kp* theory near the Γ point of the surface Brilloiun zone. A band gap size dependence of the topological insulator nanotube was studied. A comparative analysis of the topological insulator direct band gap of Bi_2Te_3 and Bi_2Se_3 nanowires as a function of radius was done. Due to high surface-to-volume ratio, a variation of nanotube geometrical sizes provides decreasing of the topological insulator band gap in 60 times compared to the corresponding bulk value. The size dependence of topological insulator nanotube band gap is mach stronger than that for the topological insulator nanowires.**

***Index Terms* — confinement, nanowire, nanotube, surface states, topological insulator.**

I. INTRODUCTION

Topological insulators (TI) in two or three dimensions have insulating energy gaps inside the finite band gap of bulk material, and gapless edge or surface states on the sample boundary that are protected by time-reversal symmetry [1]. Owing to the Kramers theorem, no time-reversal invariant perturbation can open up an insulating gap at the Dirac point on the surface. However, a topological insulator can become fully insulating both in the bulk and on the surface if a time reversal-breaking perturbation is introduced on the surface.

Inside a topological insulator, the conventional laws of electrodynamics are substantially altered, which may have applications in constructing high-temperature spintronics. Surface probe experiments using Angle-resolved Photoemission Spectroscopy (ARPES) and Scanning Tunneling Spectroscopy (STS) have provided clear evidence for existence of the theoretically predicted massless Dirac fermion surface state in Bi_2Se_3 and Bi_2Te_3 [2, 3]. However, there still exist some difficulties in probing the surface state in transport experiments because of residual bulk charge carriers. Related to disorder or unintentional intrinsic doping, the last tend to mask the surface contribution even in the cleanest samples so far available [4]. The surface contribution is easier to extract experimentally in thin-film geometries [5] or in TI nanowires [6, 7], where the surface-to-volume ratio is more advantageous.

Several standard models for both two dimensional (2D) and three dimensional (3D) TIs were constructed for quantitative predictions of the phenomena associated with the TIs. Bernevig et al. constructed a model Hamiltonian for the 2D TI in HgTe quantum wells, which demonstrates the basic mechanism of TI behavior through band inversion induced by spin-orbit coupling [8]. Zhang et al. derived a model Hamiltonian for the 3D TI Bi_2Se_3, Bi_2Te_3, and Sb_2Te_3[9]. Based on symmetry principles and a careful analysis of the relevant atomic orbitals, a full microscopic derivation of the model Hamiltonian for the 3D TI Bi_2Se_3, Bi_2Te_3, and Sb_2Te_3 was made by Liu et al.[10]. Egger et al. derived the effective low-energy theory for interacting electrons in a cylindrical nanowire made of a strong topological insulator [11].

We obtain the electronic structure of the cylindrical TI Bi_2Te_3 nanotube (NT) using the low energy approach [8, 9]. The comparison between electronic structures of TI NWs and NTs was made.

II. MODEL HAMILTONIAN

For the bulk Bi_2Te_3 (Bi_2Se_3) TI near the Γ point of the surface Brilloiun zone, Hamiltonian has the form

$$H = \varepsilon_0(\boldsymbol{k})\sigma_0\tau_0 + M(\boldsymbol{k})\sigma_0\tau_z + A_1 k_z \sigma_z \tau_x + A_2 \tau_x (k_x \sigma_x + k_y \sigma_y). \quad (1)$$

Model parameters of four bands Hamiltonian (1) have been defined in the framework of ***kp*** theory by comparison with the *ab* initio calculations [9, 10]. To find wave function of Hamiltonian (1) for a particle constrained by a ring boundaries with an external radius *b* and internal radius *a*, we use a trial function as an expansion in terms of orthonormal set of functions

$$\hat{\Psi}_j(r,\varphi,z) = \sum_{n,\sigma,\tau} K_{n,\sigma,\tau} e^{i(j-\sigma/2)\varphi} e^{ik_z z} u_{j-\sigma/2,n} \hat{\Phi} \otimes \hat{\Xi}, \quad (2)$$

where *j* is a angular momentum quantum number, Φ and Ξ set eigenvectors of σ_z and τ_z, correspondingly. Radial wave function $u_{m,n}$ has the form:

$$u_{m,n}(r) = \left(\frac{\pi}{a\sqrt{2}}\right) C_{m,n} \left(J_m(\gamma_{m,n} r/a) Y_m(\gamma_{m,n} b/a) - J_m(\gamma_{m,n} b/a) Y_m(\gamma_{m,n} r/a)\right), \quad (3)$$

where J_m abd Y_m are Bessel functions of the first and second kind, respectively, while $\gamma_{m,n}$ set roots of the equation:

$$J_m(\gamma_{m,n})Y_m(\gamma_{m,n}\,b/a)-J_m(\gamma_{m,n}\,b/a)Y_m(\gamma_{m,n})=0 \quad (4)$$

where $m=j\pm1/2$. For a small value of j, only first 2-3 roots of Eq.(4) are different, while the rest are approximately similar. The difference decreases with approaching of the external radius b to internal radius a. As a result, some energy values are degenerate at small values of both j and (b-a).

Using trial function (2) in the framework of model (1), we obtain a system of linear algebraic equations for unknown coefficients $K_{n,\sigma,\tau}$

$$\left[\varepsilon(k)+M(k)\tau-E\right]K_{n,\sigma,\tau}+A_1k\sigma K_{n,\sigma,-\tau}+ \frac{2iA_2}{a}\sum_l\frac{C_{j-\sigma/2,n}C_{j+\sigma/2,l}}{\gamma^2_{j+\sigma/2,l}-\gamma^2_{j-\sigma/2,n}}K_{n,-\sigma,-\tau}\times \left[\frac{a}{b}-\frac{Y_{j-\sigma/2}(\gamma_{j-\sigma/2,n}\,b/a)Y_{j+\sigma/2}(\gamma_{j+\sigma/2,l}\,b/a)}{Y_{j-\sigma/2}(\gamma_{j-\sigma/2,n})Y_{j+\sigma/2}(\gamma_{j+\sigma/2,l})}\right] \quad (5)$$

Coefficients ε, M, A_1, and A_2 have been defined in paper [11]. The model (5) gives adequate results if values of both external and internal NT radiuses as well as their difference are not too small.

From Eq. (5), we obtain energy spectrum of the TI Bi_2Te_3 nanotube. Using solution of model (1), electronic structure and size dependence of band gap is studied for both TI NTs and NWs. The obtained results are described in sections III and IV.

III. ELECTRONIC STRUCTURE

The Bi_2Te_3 and Bi_2Se_3 bulk materials present indirect semiconductors. The maximum of the valence band for Bi_2Te_3 and Bi_2Se_3 stays away from the Γ point, at about k_x=0.07 Å^{-1}. Since the model Hamiltonian (1) is valid in the regime $k_{x,z}$~0.04 Å^{-1}, there may be some discrepancies when we try to calculate band gap of considered TIs [10 Liu]. For the Bi_2Te_3 (Bi_2Se_3) bulk material, the bottom of the conduction band is 0.12 (0.27) eV while the top of the valence band is -0.48 (-0.28) eV at the Γ point of the Brillouin zone.

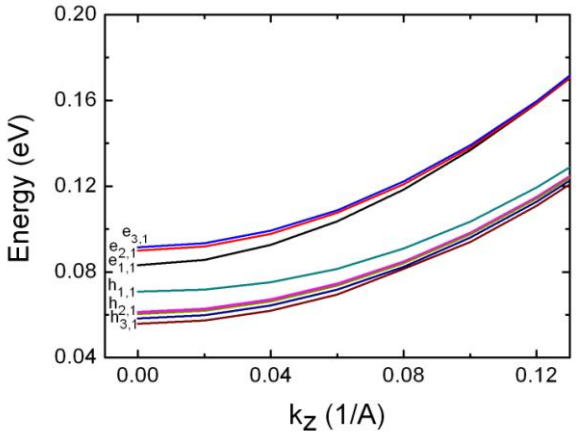

Fig.1 Electronic structure of TI Bi_2Te_3 nanotube with an external radius of 60 nm and internal radius of 10 nm. The origin is at the Γ point.

Figure 1 describes the electronic structure of the TI Bi_2Te_3 nanotube with an external radius of 60 nm and internal radius of 10 nm. Here, the first 3 (4) electron (hole) modes $e_{1,1}$, $e_{2,1}$, and $e_{3,1}$ ($h_{1,1}$, $h_{2,1}$, $h_{3,1}$, and $h_{4,1}$), corresponding to different values of angular momentum quantum number and radial quantum number being equal to 1, are presented. The origin of the graph is set at the Γ point. The Bi_2Te_3 material is an indirect band gap semiconductor, as a result, both electron and hole energy dispersion curves increase with wave vector at the vicinity of the Γ point. A splitting between the hole subbands and their dependence on ratio b/a is much greater compared to that for electrons, because the effective hole mass is less than the electron effective mass. With increasing of wave vector, the electron (hole) modes merge. The electron and hole ground states ($e_{1,1}$ and $h_{1,1}$) are located near the bottom of the conduction band of the bulk material and they are located away from other subbands.

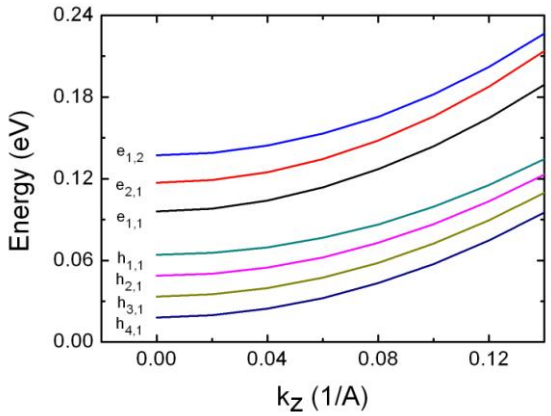

Fig.2 Electronic structure of TI Bi_2Te_3 nanowire with a radius of 10 nm. The origin is at the Γ point.

Figure 2 shows energy dispersion of the first 3 electron and 4 hole modes of the TI Bi_2Te_3 nanowire with a radius of 10 nm in the vicinity of the Γ point. The splitting of the subbands slightly decreases with wave vector. The spacing between electron (hole) subbands is about equal. For electrons, the spacing between the subbands is about 20 per cent greater than that for holes. The splitting of the subbands for NW is much greater compared to that for NT with an external radius of 60 nm and internal radius of 10 nm. The third electron mode $e_{1,2}$ corresponds to the angular momentum quantum number j=1 and radial quantum number 2. In case of the NT, the third electron mode $e_{3,1}$ corresponds to the angular momentum quantum number j=3 and the radial quantum number being equal to 1. At the origin, the band gap is 0.032 eV.

IV. SIZE DEPENDENCE OF TI DIRECT BAND GAP

For TI Bi_2Se_3 NWs, wave function and eigenvalues of Hamiltonian (1) have been obtained by Egger et al. [11 Egger]. In this case, the solution presents an expansion in

terms of Bessel function of the first kind.

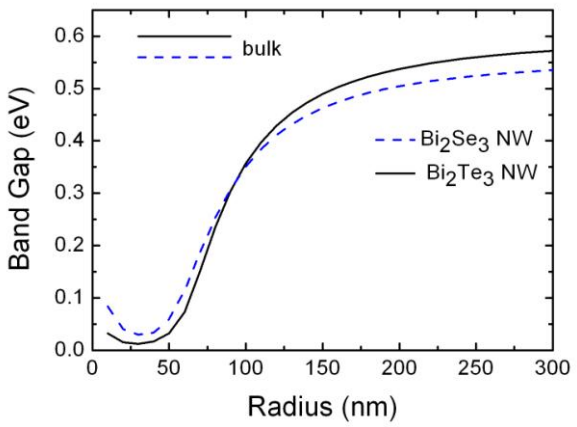

Fig.3 Dependence of the direct band gap at the Γ point of the topological insulator Bie_2Te_3 (solid line) and Bi_2Se_3 (dashed line) nanowires on radius.

Figure 3 depicts a dependence of the direct band gap at the Γ point of the TI Bie_2Te_3 and Bi_2Se_3 nanowires on radius. The band gap depends not monotonically on radius. It achieves a minimum value of 0.012 (0.03) eV at a Bi_2Te_3 (Bi_2Se_3) NW radius of 30 nm. Therefore, by adjusting NW radius, the band gap can be decreased by 50 (15) times compared to the corresponding value of 0.6 (0.56) eV at the Γ point for the Bi_2Te_3 (Bi_2Se_3) bulk material. The minimum value of the TI Bi_2Te_3 NW band gap is about twice less than the one for TI Bi_2Se_3 NW. Therefore, the TI B_2Te_3 NT is superior compared to TI Bi_2Sb_3 NT, because its band gap can be better controlled by means of variation of NW radius.

The TI NW band gap starts to change significantly with radius when the NW radius being less than 120 nm. A competition between cylindrical symmetry of the surface states and confinement effect forms a not monotonic dependence of the band gap on the radius. The cylindrical symmetry leads to a decrease of the band gap with decreasing of both NW radius and ratio bulk volume/surface area, while the confinement effect leads to an increase of the band gap, when the NW radius achieves rather small values.

Figure 4 shows dependence of the TI Bie_2Te_3 nanotube band gap on ratio *b/a* of external radius *b* to internal radius *a*. The last is taken to be equal to 10 nm. At *b/a*=8, the TI Bie_2Te_3 band gap is about 0.01 eV, which is less than the corresponding value for bulk counterpart by 60 times. The TI NT band gap starts to change significantly with ratio *a*/*b* when the last is less than 20 and the external radius is less than 200 nm. At NT external radius 30 (40) nm, the NT band gap equals 0.52 (0.55) eV, while it is equal to 0.57 eV for the 30-nm-radius Bi_2Te_3 NW. Hence, the size dependence of the TI NT band gap is more pronounced than that for the TI NW, due to the presence of both external and internal surface states in the TI NT. Hence, the influence of cylindrical symmetry of the surface states on the energy spectrum is determining in this case.

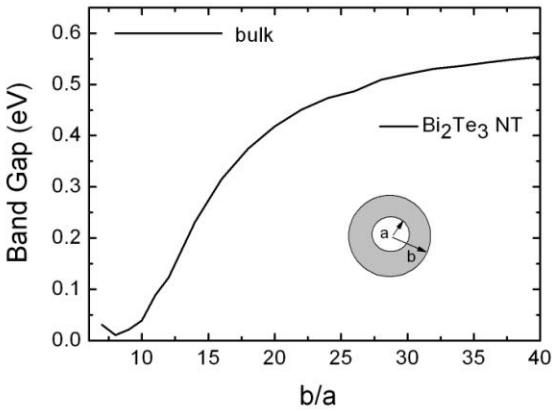

Fig. 4 Dependence of the TI Bie_2Te_3 nanotube band gap at the Γ point on ratio *b/a* of external radius *b* to internal radius *a*.

V. CONCLUSION

We studied electronic structure of TI Bi_2Te_3 NT and the corresponding band gap dependence on ratio of external-to-internal radius. A comparison between size dependences of the band gap for Bi_2Te_3 and Bi_2Sb_3 NWs as well as Bi_2Te_3 NTs was made.

For Bi_2Te_3 NTs, the electron and hole ground states ($e_{1,1}$ and $h_{1,1}$) are located near the bottom of the conduction band of the bulk counterpart and they are located away from other subbands.

The cylindrical symmetry leads to a decrease of the band gap with decreasing of both NW radius and ratio bulk volume/surface area, while the confinement effect leads to an increase of the band gap, when the NW radius achieves rather small values. The size dependence of the TI NT band gap is more pronounced than that for the TI NW, due to the presence of both external and internal surface states in the TI NT. Hence, the influence of cylindrical symmetry of the surface states on the energy spectrum is determining in this case. When the ratio of the external radius *b* to internal radius *a* of the NT is equal to 8, the TI Bie_2Te_3 NT band gap is about 0.01 eV, which is less than the corresponding value for bulk counterpart by 60 times. Therefore, the TI nanotubes are more advantageous than TI nanowires for controlling band gap.

REFERENCES

[1] J. E. Moore, "The birth of topological insulators," Nature, vol. 464, pp. 194, 2010.

[2] Y. Xia, D. Qian, D. Hsieh et al."Observation of a large-gap topological-insulator class with a single Dirac cone on the surface," Nature Physics, vol. 5, pp. 398, 2009.

[3] Zhanybek Alpichshev, J. G. Analytis, J.-H. Chu et al. "STM Imaging of Electronic Waves on the Surface of Bi2Te3: Topologically Protected Surface States and Hexagonal Warping Effects," Phys. Rev. Lett., vol. 104, pp. 016401, 2010.

[4] N. P. Butch, K. Kirshenbaum, P. Syers et al. "Strong surface scattering in ultrahigh-mobility Bi2Se3

topological insulator crystals," Phys. Rev. B, vol. 81, pp. 241301(R), 2010.

[5] A. Roth, C. Brune, H. Buhmann, L. W. Molenkamp, J. Maciejko, X. Qi, and S. Zhang, "Nonlocal Transport in the Quantum Spin Hall State," Science, vol. 325, pp. 294, 2009.

[6] H. Peng, K. Lai, D. Kong et al. "Aharonov–Bohm interference in topological insulator nanoribbons," Nature Mater., vol. 9, pp. 225, 2010.

[7] D. Kong, J.C. Randel, H. Peng et al. "Topological Insulator Nanowires and Nanoribbons," Nano Lett., vol. 10, pp. 329, 2010.

[8] B. A. Bernevig, T. L. Hughes, and S. C. Zhang, "Quantum Spin Hall Effect and Topological Phase Transition in HgTe Quantum Wells," Science, vol. 314, pp. 1757, 2006.

[9] H. Zhang, C.-X. Liu, X.-L. Qi, X. Dai, Z. Fang, and S.-C. Zhang, "Topological insulators in Bi_2Se_3, Bi_2Te_3 and Sb_2Te_3 with a single Dirac cone on the surface," Nature Phys., vol. 5, pp. 438, 2009.

[10] C.-X. Liu, X.-L. Qi, H. Zhang et al. "Model Hamiltonian for topological insulators," Phys. Rev. B, vol. 82, pp. 045122, 2010.

[11] R. Egger, A. Zazunov, A. Levy Yeyati, "Helical Luttinger Liquid in Topological Insulator Nanowires," Phys. Rev. Lett., vol. 105, pp. 136403, 2010.